JACS
JOURNAL OF THE AMERICAN CHEMICAL SOCIETY
Article
pubs.acs.org/JACS

Impact of Redox-Active Polymer Molecular Weight on the Electrochemical Properties and Transport Across Porous Separators in Nonaqueous Solvents

Gavvalapalli Nagarjuna,[§,†,⊥] Jingshu Hui,[§,‡,⊥] Kevin J. Cheng,[§,†] Timothy Lichtenstein,[§,‡] Mei Shen,[†] Jeffrey S. Moore,*[,§,†,∥] and Joaquín Rodríguez-López*[,§,†]

[§]Joint Center for Energy Storage Research, [†]Department of Chemistry, [‡]Department of Materials Science and Engineering, and [∥]Beckman Institute for Advanced Science and Technology, University of Illinois at Urbana−Champaign, Urbana, Illinois 61801, United States

Supporting Information

ABSTRACT: Enhancing the ionic conductivity across the electrolyte separator in nonaqueous redox flow batteries (NRFBs) is essential for improving their performance and enabling their widespread utilization. Separating redox-active species by size exclusion without greatly impeding the transport of supporting electrolyte is a potentially powerful alternative to the use of poorly performing ion-exchange membranes. However, this strategy has not been explored possibly due to the lack of suitable redox-active species that are easily varied in size, remain highly soluble, and exhibit good electrochemical properties. Here we report the synthesis, electrochemical characterization, and transport properties of redox-active poly(vinylbenzyl ethyl-viologen) (RAPs) with molecular weights between 21 and 318 kDa. The RAPs reported here show very good solubility (up to at least 2.0 M) in acetonitrile and propylene carbonate. Ultramicroelectrode voltammetry reveals facile electron transfer with $E_{1/2}$ ∼ −0.7 V vs Ag/Ag$^+$(0.1 M) for the viologen 2+/+ reduction at concentrations as high as 1.0 M in acetonitrile. Controlled potential bulk electrolysis indicates that 94−99% of the nominal charge on different RAPs is accessible and that the electrolysis products are stable upon cycling. The dependence of the diffusion coefficient on molecular weight suggests the adequacy of the Stokes−Einstein formalism to describe RAPs. The size-selective transport properties of $LiBF_4$ and RAPs across commercial off-the-shelf (COTS) separators such as Celgard 2400 and Celgard 2325 were tested. COTS porous separators show ca. 70 times higher selectivity for charge balancing ions ($Li^+BF_4^-$) compared to high molecular weight RAPs. RAPs rejection across these separators showed a strong dependence on polymer molecular weight as well as the pore size; the rejection increased with both increasing polymer molecular weight and reduction in pore size. Significant rejection was observed even for r_{poly}/r_{pore} (polymer solvodynamic size relative to pore size) values as low as 0.3. The high concentration attainable (>2.0 M) for RAPs in common nonaqueous battery solvents, their electrochemical and chemical reversibility, and their hindered transport across porous separators make them attractive materials for nonaqueous redox flow batteries based on the enabling concept of size-selectivity.

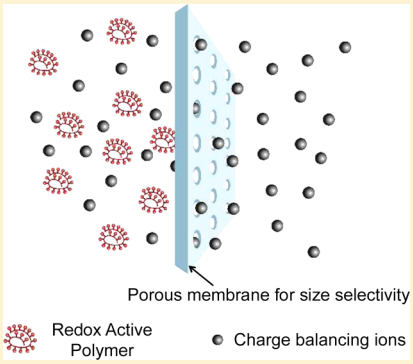

1. INTRODUCTION

Redox flow battery technology offers many advantages for grid energy storage such as load-leveling, long durability, flexible operation, easy scalability, high-efficiency, and low cost.[1−3] In this technology, electrochemical energy is stored in highly concentrated solutions of reversible redox-active molecules and separated in compartments for the low and high electrochemical potential species. Nonaqueous redox flow batteries (NRFBs) are a potentially viable alternative to their aqueous counterparts (ARFBs) having a wide range of redox-active species and electrolytes available for their design.[1,4−6] The energy density of NRFBs can be dramatically increased by using redox couples that are highly soluble in organic solvents and that operate at electrode potentials well beyond the window of stability of aqueous electrolytes.[7] Despite these exciting prospects, the lower ionic conductivity observed in nonaqueous electrolytes has prevented the wide-scale development of NRFBs.

Challenges in adapting commonly used ion exchange membranes (IEMs) as separators from aqueous to nonaqueous environments are greatly responsible for the paucity in studies of NRFBs.[4,8−11] The role of the separator is to physically and electronically isolate the high and low potential redox species compartments. This prevents the mixing of the redox-active components (crossover) and simultaneously provides high electrolyte ionic conductivity for minimizing losses due to resistance to current flow.[3,4] Using IEMs designed for aqueous environments, many of which are proton conductors, decreases the power density of NRFBs by 1 order of magnitude

Received: August 19, 2014
Published: October 17, 2014

dx.doi.org/10.1021/ja508482e | J. Am. Chem. Soc. 2014, 136, 16309−16316

compared to ARFBs.[4] Moreover, IEMs are expensive, and they contribute to ∼20% of the battery cost.[12,13]

Finding improvements in the performance of IEM's is an active research area,[4] but we reasoned that an alternative for NRFBs could be based on electrolyte size-selectivity[14] rather than ionic-selectivity. Size-selectivity using nanoporous membranes has been introduced recently in aqueous vanadium redox flow batteries for separating proton transport from that of larger vanadium cations.[4,15] A strong emphasis is placed on the complex design of these membranes so they can adjust their sterics and electrostatics to effectively discriminate the redox-active species.[12,16−20] Here, we introduce an alternate approach in which the size of the redox-active species is varied and systematically studied through a chemically flexible synthetic polymer approach. This strategy de-emphasizes membrane design and enables an insightful exploration of the properties of potential redox-active candidates.

Unlike IEMs, porous membranes transport molecules based on size. Thus, by careful design of the redox-active component for matching an appropriate size, one can take advantage of size exclusion to selectively and efficiently transport charge-balancing ions across the porous membrane while retaining the active species in its compartment. Commercial off-the-shelf (COTS) porous separators are relatively inexpensive compared to IEMs,[13] hence their utilization in NRFBs could in principle bring down the overall cost of the NRFBs. Although porous separators have been widely used in lithium-ion batteries,[13] their use in NRFBs is not well explored.[4,15] This could be due to the lack of development in redox-active components whose size is easily varied without adversely affecting their electrochemical properties.

Controlling the molecular weight of redox-active polymers (RAPs) is an easy way to vary the size of the redox-active components. Understanding the size-dependent transport, solubility, and electrochemical properties of RAPs may enable their use in conjunction with COTS porous membranes as separators in NRFBs.[3,4] To the best of our knowledge, there are no known RAPs with the desired solubility, energy density, and (electro)chemical reversibility in NRFBs. Poly(vinyl ferrocene)[21,22] and poly(vinyl anthracene)[23] are well-studied RAPs for benchmarking the properties of soluble macromolecular designs. In this study, we focused on the synthesis of viologen-based RAPs of different molecular weight and studied the impact of polymer molecular weight on their electrochemical, solubility, viscosity, and transport properties across commercial porous membranes as a means for enabling size-selectivity for NRFBs.

2. EXPERIMENTAL SECTION

2.1. Materials and Experimental Techniques. Poly(vinylbenzyl ethyl viologen) polymers (**RAPs 1−5**, Scheme 1) of five different molecular weights (M_n = 21, 104, 158, 233, and 318 kDa) were synthesized starting from poly(vinylbenzyl chloride) (PVBC). Typical synthesis of RAPs involved heating a mixture of PVBC and ethyl viologen in dimethylformamide, followed by anion exchange with ammonium hexafluorophosphate. The resultant polymers were isolated and purified via precipitation. Quantitative functionalization of poly(vinyl benzyl chloride) with ethyl viologen was confirmed by ^{1}H NMR, ATR-IR, UV−vis absorption spectra, and elemental analyses (see Supporting Information). PVBC of molecular weight = 5.3, 60, and 82 kDa were purchased from Polymer Source. The 27 and 41 kDa PVBC polymers were synthesized using reversible addition−fragmentation chain-transfer (RAFT) polymerization.[24] The corresponding viologen monomer was also synthesized for comparison (Scheme 1).

Scheme 1. Chemical Structures of (a) Monomer and RAPs 1−5 and (b) Reduction Reaction

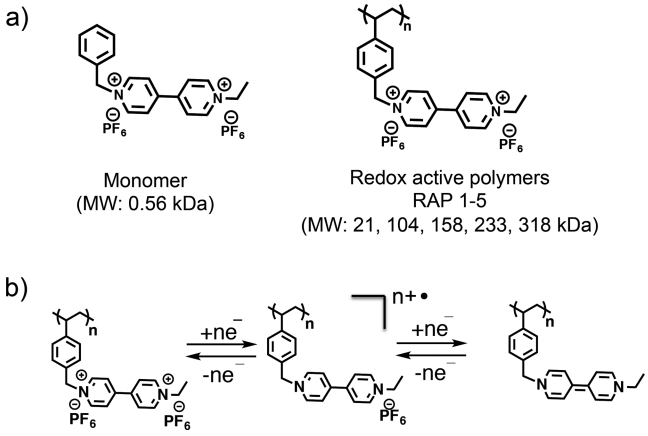

RAPs 1−5 were characterized using ^{1}H NMR, ATR-IR, and elemental analysis. The viscosities of the **RAPs 1−5** were measured using parallel plate rheometry at different concentrations from 0.01 to 1.0 M in acetonitrile. UV−vis absorption spectra were recorded in acetonitrile at different concentrations to determine the molar absorption coefficient of the polymers. For all the studies, polymer concentration is defined as moles of repeat unit per liter. Polymer transport measurements across porous COTS separators were carried out at 0.01 M using PermeGear side-bi-side cell in which the separator was sandwiched between the donor (containing polymer solution) and receiver (containing acetonitrile) cells.[4] Both solutions were stirred for 24 h to allow the polymer to crossover into the receiver compartment. After 24 h, the concentration of RAP in the receiver cell was determined using UV−vis absorption spectroscopy, and the percent polymer rejection was calculated (see Supporting Information for details). The diffusion of $LiBF_4$ under similar conditions was determined from its conductance.

2.2. Electrochemical Methods. All electrochemical experiments were performed on a CHI920D potentiostat and inside of an Ar-filled drybox with stringent control of O_2 and moisture levels. All chemical reagents, except for synthesized RAPs, were purchased from Sigma-Aldrich with the highest available purity and used as received. Unless specified, all voltammetric and bulk electrolysis experiments were carried out using a standard three-electrode configuration with either a large-area Pt mesh (bulk electrolysis), 12.5 μm radius Pt ultramicroelectrode (UME), or 1.15 mm radius Pt disk electrode (transient voltammetry) as the working electrode, a nonaqueous Ag/Ag^+ reference electrode (CHI112, 0.1 M $AgNO_3$ in acetonitrile solution), and a graphite rod as counter electrode. Most experiments were carried out in a three-chamber electrochemical cell with 1.6 μm glass frits. The transient voltammetry of viologen polymers was tested with a 10 mM effective concentration of repeating units for all **RAPs 1−5** in 0.1 M $LiBF_4$ in acetonitrile as supporting electrolyte and using a 1.15 mm Pt disk as working electrode. Multiple scan cycles were performed until an adsorbed film of the RAP was deposited and stable. After rinsing several times with acetonitrile, Pt disk electrodes were immersed into blank 0.1 M $LiBF_4$ in acetonitrile electrolyte to test RAP adsorption at different scan rates.

The chemical stability and charge storage properties of RAPs were studied by bulk electrolysis (BE), by holding a Pt mesh working electrode at a constant potential while stirring at a constant rate and recording the current and charge passed through the system. We used an initial concentration of 10 mM **RAPs 1−5** in 0.1 M acetonitrile solution. All solutions started from the 2+ viologen form. The Pt mesh was held at −0.9 V for BE reduction (2+/+) and at −0.3 V for BE oxidation (+/2+). The second viologen reduced state (+/0) was accessed by holding the Pt mesh at −1.4 V. Steady-state UME

dx.doi.org/10.1021/ja508482e | J. Am. Chem. Soc. 2014, 136, 16309−16316

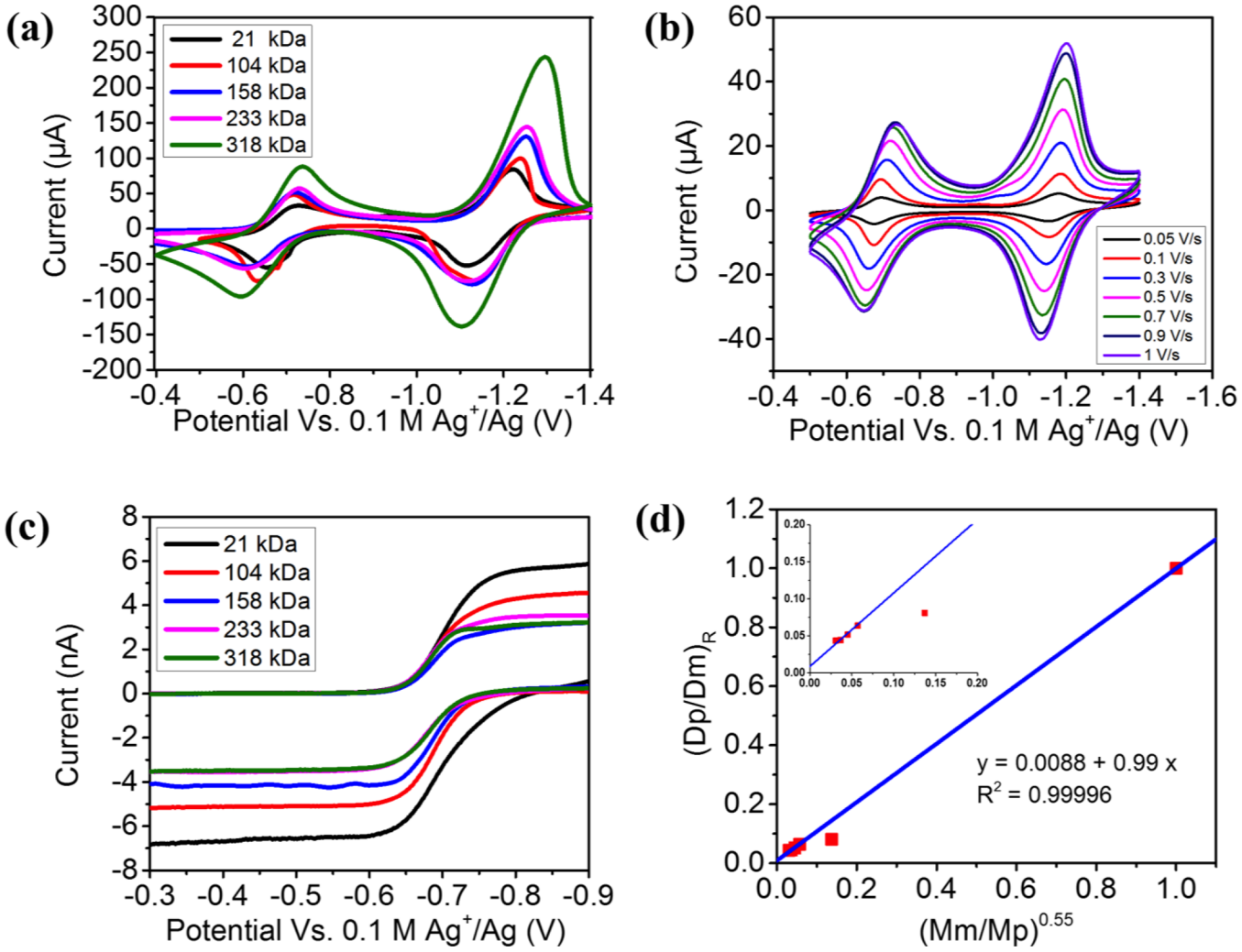

Figure 1. Electrochemical characterization of **RAPs 1−5**. (a) Cyclic voltammograms of **RAPs 1−5** on 0.04 cm^2 Pt disk electrode (ν = 100 mV/s). (b) Voltammetry of adsorbed **RAP 1** on 0.04 cm^2 Pt disk electrode in blank supporting electrolyte. (c) Steady-state voltammograms of **RAPs 1−5** at 12.5 μm Pt UME (ν = 10 mV/s) for the original and reduced form. (d) Plot of monomer-normalized diffusion coefficient vs molecular weight for **RAPs 1−5**. Inset shows zoom of polymer high molecular weight region. In all experiments, RAP concentration was 0.01, and 0.1 M $LiBF_4$ in acetonitrile was used as supporting electrolyte solution.

voltammograms were obtained before and right after bulk electrolysis with 12.5 μm Pt tip as working electrode. The time-dependent evolution of + viologen electrolytes was followed by tracking the steady-state voltammograms approximately every 10 min after BE until an unchanging limiting current was recorded.

The UME limiting current of monomer and polymers at high concentration were studied for the 2+/+ reductive process. A small portion (~100 μL) of 1.0 M monomer of RAPs solution in acetonitrile was used as the starting material, and then different volumes of 0.5 M $LiBF_4$ in acetonitrile solution were added for diluting to different concentrations. These measurements were achieved on the small volumes through a two-electrode configuration using a Pt wire wrapped around the UME as counter electrode.

3. RESULTS AND DISCUSSION

3.1. Characterization of RAPs 1−5. The percent functionalization of PVBC with ethyl viologen was determined using ^{1}H NMR, ATR-IR, UV−vis absorption spectra, and elemental analyses. In PVBC, ν_{CH_2Cl} stretch[25] appears at 1280 cm^{-1}. ATR-IR spectra (Figure S1) of **RAPs 1−5** show a complete disappearance of the peak at 1280 cm^{-1} and also display the peak corresponding to the viologen quaternary amine[25] ($\nu_{>N+<}$) at 1650 cm^{-1}. For a given concentration of repeat units, the molar extinction coefficients of RAPs (Table S4) were found to be close to that of monomer, indicating the near-quantitative substitution of PVBC with ethyl viologen.[1]H NMR, elemental analyses (C, H, N, P, F, and Cl shown in Table S2), and bulk electrolysis (see below) data further support the near-quantitative functionalization of PVBC with ethyl viologen.

RAPs 1−5 display good solubility in nonaqueous electrolytes such as acetonitrile and propylene carbonate, both commonly used solvents in NRFBs.[1,4] The 21 kDa polymer is soluble up to 2.9 M in acetonitrile, while the highest molecular weight 318 kDa polymer is soluble up to 2.1 M (Table S1). The monomer showed negligible change in viscosity with an increase in concentration from 0.01 to 1.00 M, whereas the viscosity of polymer solutions increased with increasing molecular weight and concentration (Figure S2 and Table S3). UV−vis absorption spectra of monomer and polymers were recorded in acetonitrile at different concentrations, and their molar absorption coefficients were determined (Figures S3 and S4). The similarity between the absorption spectra of the polymers

dx.doi.org/10.1021/ja508482e | J. Am. Chem. Soc. 2014, 136, 16309−16316

Table 1. Summary of Electrochemical Characterization and Transport Properties of RAPs 1−5

molecular weight (kDa)	radius of RAPs (nm)	diffusion coefficient of original state (10^{-10} m^2/s)	diffusion coefficient of reduced state (10^{-10} m^2/s)	rejection across Celgard 2400 membrane	rejection across Celgard 2325 membrane	permeability (10^{-12} m^2/s)	percent electroactive units (%)
0.56	0.35	13.9	16.8	4.8 ± 0.5	3.1 ± 2.6	14.82 ± 1.00	100
21	4.1	1.22	1.36	45.9 ± 0.4	84.6 ± 0.9	3.95 ± 0.50	96
104	5.1	0.95	1.07	72.0 ± 2.9	81.1 ± 1.9	3.53 ± 0.03	98
158	7.2	0.67	0.87	80.9 ± 0.7	86.3 ± 2.7	1.76 ± 0.20	94
233	6.5	0.73	0.74	81.0 ± 2.1	88.5 ± 0.3	2.10 ± 0.50	96
318	7.1	0.66	0.73	86.3 ± 0.5	92.8 ± 0.7	2.06 ± 0.30	96

and monomer (Figure S4) suggests that there is minimal intrachain and interchain interaction between viologens in polymer solution.[23,26] This interpretation is also supported by the electrochemical data shown below.

3.2. Electrochemical Characterization of RAPs 1−5. We chose a viologen-based macromolecular design[27−30] since the monomeric units have a small molecular footprint, are highly soluble in polar solvents, show appealing reduction potentials, and undergo facile electron transfer with chemical reversibility.[31,32] This combination of properties makes them well-suited as low potential redox species in NRFBs as they promise high energy density, high stability during cycling, and minimal electrode kinetics losses.

Transient voltammetry of 10 mM solutions of **RAPs 1−5**, shown in Figure 1a, was recorded in acetonitrile with 0.1 M $LiBF_4$ as a supporting electrolyte using a 1.15 mm radius Pt electrode. The shape of these voltammograms suggests a mixed adsorptive and diffusive behavior for all tested polymers. In general, two clearly defined reductive processes are observed at ca. −0.7 and −1.2 V vs 0.1 M Ag^+/Ag. For comparison, the monomer exhibits two Nernstian waves at similar potentials and with similar separation between the first (2+/+) and second (+/0) reductions (Figure S5). In addition to this similarity, the current intensities for different polymers at the same effective concentration of redox pendants are comparable and do not show a strong dependence on molecular weight. These results suggest that viologen motifs do not interact electronically through the polymer backbone, in agreement with results from UV−vis spectroscopy, and that the redox characteristics of **RAPs 1−5** are essentially the same as that displayed by the monomer.

In contrast to the monomer, adsorption is likely to be observed in **RAPs 1−5** because of a larger cross-section for interaction between the negatively charged electrode and the positively charged polymer as well as other physisorption interactions. Pt electrodes exposed to solutions containing **RAPs 1−5** were carefully rinsed and transferred to blank electrolyte to confirm irreversible adsorption. The resulting voltammograms displayed the behavior associated with an adsorbed electroactive layer, as shown in Figure 1b for **RAP 1**, where both reduction voltammetric peak currents increase proportionally to the scan rate (Figure S6).[33,34] The surface density of redox-active groups was estimated to be ca. 100−200 μC/cm^2 for **RAP 1**, which is at least 1 order of magnitude larger than a conservative estimate of a monolayer based on the molecular footprint and loading of the polymer (10 μC/cm^2). Electrode surface roughness and limited electrostatic interactions with the electrode are possible causes of multilayer formation. Electrochemical data show evidence of charge transport in this polymer layer. A smaller peak splitting and larger intensity observed for the +/0 process in comparison to the 2+/+ are consistent with a larger rate of self-exchange for the viologen +/0 redox couple as has been observed in other polymer films, including those based on viologen.[35,36] Despite irreversible adsorption, the film formed by **RAPs 1−5** is electroactive and allows solution-based polymer molecules to engage in facile electron transfer and complete bulk reduction as demonstrated by microelectrode and chronocoulometric experiments described below.

Steady-state voltammetry using UMEs was used to selectively study the diffusion behavior of **RAPs 1−5**. At small electrodes, the increase in the mass transfer coefficient of solution species masks the contribution from transient surface processes when voltammetry is conducted at low scan rates. Figure 1c shows the UME voltammetry at 10 mV/s for both the reduction of the fully oxidized (2+) and for the oxidation of the singly reduced (+) forms of **RAPs 1−5**. These voltammograms show a characteristic sigmoid shape and few indications of kinetic complications as evidenced by their width and correspondence between the position of the cathodic and anodic curves. Despite the possibility of radical-initiated reactions during the transformation of viologen 2+ to the monovalent radical cation +, the position and intensity of the oxidation and reduction waves indicate no profound chemical changes in the sample as the midway potentials, $E_{1/2}$, remain unchanged. Although the limiting current for the oxidation of the + form is consistently slightly higher than that for the reduction of 2+, the similarity between their values suggests a facile and quantitative transformation of either form at the electrode surface. The mass transfer limiting current is estimated as $i_{lim} = 4nFaDc^*$ where $n = 1$, $F = 96{,}485$ C/mol, $a = 12.5$ μm, D is the apparent diffusion coefficient of viologen motifs, and c^* is their concentration in the bulk. The diffusion coefficient of viologen groups in **RAPs 1−5** is deduced from i_{lim} for both original and reduced states. The diffusion coefficient values at concentrations 10 mM are shown in Table 1. In general, smaller diffusion coefficients were observed as the molecular weight of the polymer increased. The ratio of the diffusion coefficient of polymer to monomer, D_p/D_m varies linearly with respect to the 0.55 power of the ratio of molecular weight of monomer and polymer, $(M_m/M_p)^{0.55}$, as plotted in Figure 1d for the + and Figure S7 for the 2+ form. This behavior has been empirically observed for noninteracting redox centers in ferrocene redox polymers and explains the decrease in limiting current as a consequence of the impact of molecular weight on the diffusion coefficient following the behavior predicted by the Stokes−Einstein equation.[22] This result allows us to confidently estimate the diffusion coefficients shown in Table 1 and strongly suggests the noninteracting and quantitative transformation of viologen groups in **RAPs 1−5** regardless of their size.

3.3. Charge Storage in RAPs. **RAPs 1−5** display excellent charge storage properties, which make them suitable for NRFBs. Figure 2 and its inset show results for the potential-

dx.doi.org/10.1021/ja508482e | J. Am. Chem. Soc. 2014, 136, 16309−16316

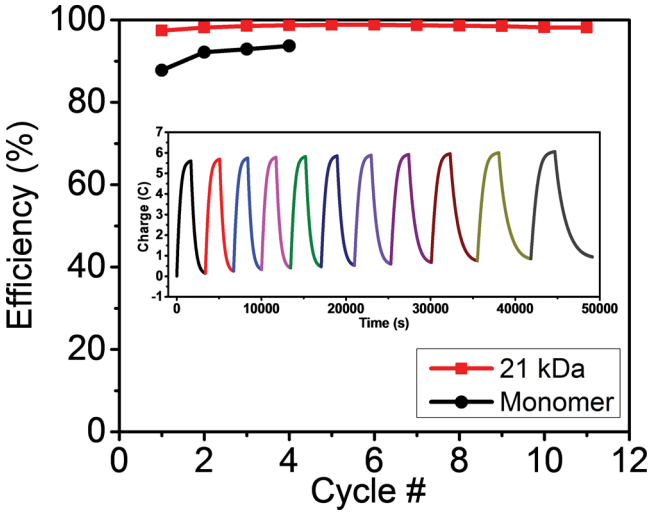

Figure 2. Charge storage properties of monomer and **RAP 1** (21 kDa). Inset shows 11 cycles of potential-controlled bulk electrolysis of 6 mL 10 mM **RAP 1** in 0.1 M $LiBF_4$ acetonitrile using a Pt mesh working electrode. Pt mesh was held at −0.9 V for BE reduction (2+/+) and at −0.3 V for BE oxidation (+/2+). The charge cycling efficiencies were calculated as the ratio of BE oxidation to BE reduction for each cycle.

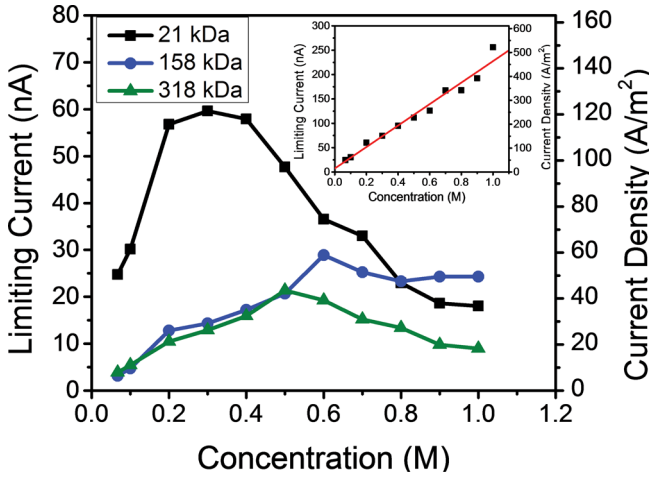

Figure 3. Diffusion-limited steady-state current change of selected RAPs at high concentration obtained using a 12.5 μm Pt UME in 0.5 M $LiBF_4$ as supporting electrolyte. Inset shows the expected limiting current for **RAP 1** if corrected for viscosity effects as shown in Figure S2.

controlled bulk electrolysis over multiple cycles for the 21 kDa polymer for the 2+/+ redox transformation. While there is a small decrease in the initial charge capacity (Table S5), no further signal decrease attributable to decomposition is observed upon consecutive cycles. Preliminary UME experiments conducted on the reduced form of **RAPs 1−5** obtained by bulk electrolysis did show a decrease in their steady-state current over a 2−4 h period (Figure S8), however NMR and UV−vis spectrophotometry did not reveal strong evidence of sample decomposition. We believe that a slow aggregation process of the reduced polymer molecules is responsible for this observation; however, this does not affect their charge storage capacity. Indeed, **RAP 1** displays a stable >97% cycling efficiency throughout 11 cycles, which is higher than monomer efficiency (Figure 2) under the same experimental conditions. Bulk electrolysis experiments also showed that at least 94% of the nominal viologen loading on **RAPs 1−5** is accessed electrochemically, thus confirming the quantitative UME voltammetry results and strongly suggesting that solution-based RAPs are versatile charge storage media for NRFBs. Table 1 summarizes the result of our systematic electrochemical analysis of **RAPs 1−5**.

For applications in NRFBs, achieving a high concentration of charge storage material is crucial for attaining a practical charge capacity. All five polymers are highly soluble in acetonitrile and propylene carbonate. We tested samples with concentrations up to ∼1 M. Using UME voltammetry to minimize solution resistive potential drop, the electrochemical activity of **RAPs 1−5** was studied in the high concentration regime as shown in Figure 3. The diffusion-limited steady-state current increased with the polymer concentration until reaching a certain maximum (0.3 M for 21 kDa, 0.6 M for 158 kDa, and 0.5 M for 318 kDa) and decreased at higher concentration. This behavior has been observed in highly concentrated solutions of organic species.[37,38] We tested the hypothesis that this decrease was due to an increase in solution viscosity (Figure S2) which in turn affected the diffusion coefficient. The inset of Figure 3 shows the prediction of the limiting current for **RAP 1** at the UME if the experimental limiting currents are corrected for the increase in viscosity using an analogue of Walden's rule (similar plots can be obtained for other RAPs, Figure S9). The observed linearity in this plot suggests that even at the most concentrated solutions, similar electrode processes to those observed in dilute 10 mM solutions apply, despite the possibility of multiple intermolecular and ion migration effects at high concentrations.[37,38] Likewise, it is noteworthy that the concentrated solutions remain highly electroactive and able to support a steady-state current, both properties are highly desirable for NRFBs, and that indicate a lack of observed solution decomposition and electrode fouling. On the other hand, the decrease in current might suggest that increasing the charge capacity and energy density of a solution by concentrating RAPs implies a trade-off in the power density if used in NRFBs.

Another strategy to increase the charge capacity of **RAPs 1−5** is to access the second reductive process. Preliminary experiments on **RAP 1** showed that bulk electrolysis from the 2+ directly to the 0 states results in a recovery of only about 61% of theoretical charge (Figure S10). Our laboratories are currently investigating ways to improve this charge utilization. While Figure 3 evidences complex interactions between the rheological and electrochemical properties of RAPs in solution, in practical terms, an attainable volumetric energy density of up to 14 Ah/L as well as their electrochemical and chemical reversibility make them suitable candidates for NRFBs.

3.4. Size-Based Selectivity of COTS Porous Separators. In the case of IEMs, the selectivity for ions is mainly due to their charge, whereas in porous separators the selectivity is based on size.[4,39] To study the size-based selectivity of COTS porous separators for charge balancing ions compared to RAPs, permeability of $LiBF_4$, monomer, and RAPs across porous separators was determined from time dependent transport studies (Figures 4a and S11). Time-dependent transport across Celgard 2325 (pore radius = 14 nm) at 0.01 M was carried out using PermeGear side-bi-side cell. The solution in the receiver cell was flowed through a cuvette, and the absorbance at absorption maximum was recorded at regular intervals to determine the crossed over monomer and polymer concen-

dx.doi.org/10.1021/ja508482e | J. Am. Chem. Soc. 2014, 136, 16309−16316

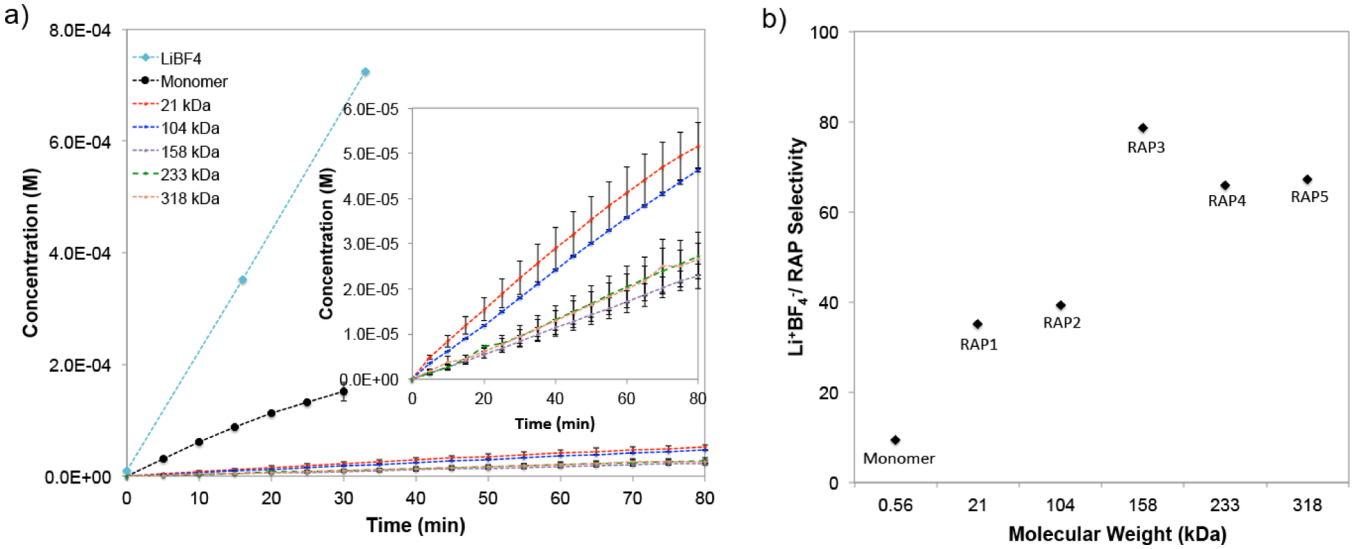

Figure 4. (a) Time-dependent transport of $LiBF_4$, monomer, and **RAPs 1−5** across Celgard 2325 at 0.01 M. Inset shows the **RAPs 1−5** region of the plot. (b) Size-based selectivity of Celgard 2325 for Li^+BF4^- compared to monomer and **RAPs 1−5**.

trations.[4,40] Time-dependent transport of $LiBF_4$ was determined from its conductance (Figure S12). The initial linear region of the time dependent transport curves was used to calculate the permeability of RAPs (see Supporting Information for details) and is reported in Table 1. $LiBF_4$ showed a steep increase in concentration with time, indicating its faster transport across the separator compared to the monomer and RAPs. While permeability of $LiBF_4$ (138.5×10^{-12} m^2/s) is only 9 times higher than that of the small molecule monomer, it is ca. 70 times higher than that of high molecular weight RAPs (Figure 4b). For vanadium flow batteries, only 15 times higher selectivity was observed for proton permeation compared to vanadium with porous separators;[15] the porous separators were modified with silica to increase the proton selectivity to 50 times.[18] Gratifyingly, for the high molecular weight RAPs studied here, COTS porous separators show ca. 70 times higher selectivity for charge balancing ions ($Li^+BF_4^-$) compared to RAPs. This observation clearly demonstrates the advantage of using RAPs, instead of small molecules, as charge storage materials for size-selective transport in porous separators. RAPs also showed negligible adsorption onto the COTS porous separators (Table S7).

We now turn to evaluate the impact of RAPs molecular weight on their transport properties across porous separators. For macromolecular transport across porous separators, the steric partition coefficient, i.e., the ratio of macromolecule concentration inside the pore and bulk solution, is known to play a key role in both size-exclusion chromatography and ultrafiltration.[41−48] Steric partition coefficient depends on the relative macromolecular size as defined by the size ratio of the macromolecule relative to the pore size. Theoretical models for linear polymers predict a decrease in steric partition coefficient with increase in relative polymer size; only 20% of polymers can access the pore volume for a relative polymer size of 0.33, and polymers are completely size excluded from entering the pore for relative sizes >0.6 (Figure S13).[41,43] Other factors such as hindrance to polymer diffusion inside the pores as well as the polymer shape and charge might also influence the polymer transport across porous separators.[48−51]

Relative polymer size-dependent (r_{poly}/r_{pore}) RAPs rejection across COTS separators is shown in Figures 5 and S14.

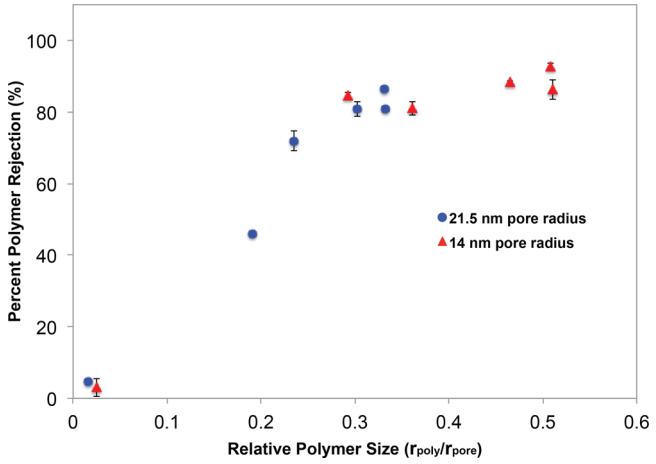

Figure 5. Relative polymer size-dependent polymer rejection across COTS porous separators for **RAPs 1−5**.

Polymer size (solvodynamic radius) was determined using Stokes−Einstein equation (Table S6), and is shown in Table 1. Polymer size increased with increasing molecular weight up to 158 kDa, and no significant change was observed with further increase in molecular weight. Relative polymer size of the RAPs increased up to 0.33 and 0.50 for larger (Celgard 2400, 21.5 nm pore radius) and smaller (Celgard 2325, 14 nm pore radius) pore size membranes, respectively. As can be seen from Figure 5, the percent polymer rejection is seen to increase with increasing r_{poly}/r_{pore}. The percent polymer rejection increased rapidly until r_{poly}/r_{pore} of 0.3 and then showed a gradual increase after that. The impact of relative polymer size on percent rejection is more apparent for 21 kDa (**RAP 1**) polymer. For larger pore radius membrane, **RAP 1** showed only 46% rejection while for smaller pore radius membrane ca. 85% rejection is obtained. ca. 80% rejection is observed for all the RAPs as r_{poly}/r_{pore} approaches 0.3, which is in close accordance with the theoretically expected[41] steric exclusion for linear polymers across porous separators. We believe that the loss of conformational freedom for polymers inside the pores even for the relative polymer sizes smaller than the pore size is the main

dx.doi.org/10.1021/ja508482e | J. Am. Chem. Soc. 2014, 136, 16309−16316

reason for the observed steric hindrance involved in the size-based separation of RAPs across COTS porous membranes. Among all the studied RAPs, the higher molecular weight polymer **RAP 5** showed the highest percent polymer rejection (93%) across the smaller pore radius membrane. In the case of widely studied vanadium aqueous flow batteries with Nafion 115 as the separator, there is 12% crossover of vanadium, and the crossover increases depending on the cell operating conditions.[52,53] Polymer crossover of as low as 7% (93% rejection) is achieved with the RAPs studied here, which suggests that it is possible to realize high Coulombic efficiency using RAPs in conjunction with porous separators in flow batteries.

Complete rejection of the polymers can be realized with RAPs that have higher r_{poly}/r_{pore} values (>0.6). However, based on the electrochemical studies, it is shown that higher molecular weight polymers have low limiting current as shown in Figure 3. Thus, although high molecular weight RAPs offer higher rejection across the porous separators, there will be a trade-off in electrochemical properties such as limiting current. Other macromolecular architectures such as star, branched, and cyclic polymers will be very interesting to vary the relative polymer size and obtain higher polymer rejection without adversely impeding their electrochemical properties.

Given the low crossover observed for RAP 5, we tested preliminarily its charge/discharge performance in a proxy setup for a nonaqueous flow cell. This consisted of two stirred electrolyte compartments with a Celgard 2325 separator sandwiched between them. The open circuit voltage of the cell was 1.11 ± 0.05 V (three different cells), which is in good agreement with the 1.27 ± 0.05 V predicted from the initial state of charge of the **RAP 5** solution and a metal oxide auxiliary electrode (Table S8). Electrolytic conductivity through the Celgard separator allowed the charge/discharge of this cell in $LiBF_4$ electrolyte as shown in Figures S15 and S16, where stable operation over multiple cycles was observed at C/10 rate. The resulting curves displayed one monotonic and well-defined plateau on the first cycles, corresponding to the conversion of the viologen +/2+ redox pair, and stable operation in subsequent cycles. Furthermore, Figure S17 and Table S9 show that the Celgard separator retained its mechanical integrity and that the low crossover observed in the diffusion cell studies was maintained during prolonged periods of operation even for mixed solutions of viologen +/2+. This preliminary evaluation highlights the potential for using the size-selective strategy enabled by COTS and RAP electrolytes in a practical redox flow cell. We showed that this leads to an operating cell with substantially decreased redox-active component crossover.

4. CONCLUSIONS

We have shown that size-based selective transport of supporting electrolyte ($Li^+BF_4^-$) across COTS porous separators is attainable by controlling the size of the charge storage material. Viologen-based redox-active polymers **RAPs 1−5** of molecular weight between 21 and 318 kDa were synthesized to vary the size of the charge storage material. The molecular weight dependent RAPs electrochemical properties and transport across porous separators were studied. Although transient voltammetry showed the presence of multilayer RAP adsorption on Pt electrodes from low concentration solutions of **RAPs 1−5** (10 mM), ultramicroelectrode voltammetry revealed facile electron transfer with $E_{1/2} \sim -0.7$ V vs Ag/Ag^+ for the viologen 2+/+ reduction at concentrations as high as 1.0 M in acetonitrile. Controlled potential bulk electrolysis indicates that 94−99% of the nominal charge on different RAPs is accessible, and the electrolysis products are stable upon cycling. While at high concentration the limiting current of RAPs in solution is decreased due to a concurrent increase in solution viscosity, **RAPs 1−5** preserve most of the desirable electrochemical properties of the originating viologen-based monomer such as high solubility, similar redox potential, and their electrochemical and chemical reversibility. This makes them suitable candidates for low potential species in NRFBs.

Selectivity for $Li^+BF_4^-$ transport across COTS porous separators increased significantly by changing the charge storage material from small molecule monomer (9 times) to redox-active polymers (ca. 70 times). The percent polymer rejection across the COTS separator increased with increase in RAP molecular weight as well as reduction in pore size. Polymer crossover of as low as 7% (93% rejection) was achieved with the RAPs studied here.

Our systematic studies show a complex relationship between polymer molecular weight and electrochemical, rheological, and transport properties. Nonetheless, they establish the feasibility of the size-selective separator approach aided by redox-active polymers to explore new prospects in NRFBs. We preliminarily showed that this combination of elements can lead to an operating cell with adequate performance and substantially decreased redox-active component crossover. We are currently exploring other highly soluble redox-active components as well as other macromolecular architectures such as star, branched, and cyclic polymers that will be of interest for tuning polymer size, transport, and electrochemical properties for enhanced NRFB performance.

■ ASSOCIATED CONTENT

Ⓢ Supporting Information

Synthesis, physical properties, chemical characterization, electrochemical characterization, and methods used for transport studies of **RAPs 1−5** are presented. This material is available free of charge via the Internet at http://pubs.acs.org.

■ AUTHOR INFORMATION

Corresponding Authors

jsmoore@illinois.edu
joaquinr@illinois.edu

Author Contributions

⊥These authors contributed equally.

Notes

The authors declare no competing financial interest.

■ ACKNOWLEDGMENTS

This work was supported as part of the Joint Center for Energy Storage Research, an Energy Innovation Hub funded by the U.S. Department of Energy, Office of Science, Basic Energy Sciences.

■ REFERENCES

(1) Brushett, F. R.; Vaughey, J. T.; Jansen, A. N. *Adv. Energy Mater.* **2012**, *2*, 1390−1396.

(2) de Leon, C. P.; Frias-Ferrer, A.; Gonzalez-Garcia, J.; Szanto, D. A.; Walsh, F. C. *J. Power Sources* **2006**, *160*, 716−732.

(3) Weber, A. Z.; Mench, M. M.; Meyers, J. P.; Ross, P. N.; Gostick, J. T.; Liu, Q. *J. Appl. Electrochem.* **2011**, *41*, 1137−1164.

(4) Shin, S.-H.; Yun, S.-H.; Moon, S.-H. *RSC Adv.* **2013**, *3*, 9095−9116.
(5) Alotto, P.; Guarnieri, M.; Moro, F. *Renewable Sustainable Energy Rev.* **2014**, *29*, 325−335.
(6) Darling, R. M.; Gallagher, K. G.; Kowalski, J. A.; Ha, S.; Brushett, F. R. *Energy Environ. Sci.* **2014**, DOI: 10.1039/C4EE02158D.
(7) Wang, Y.; He, P.; Zhou, H. *Adv. Energy Mater.* **2012**, *2*, 770−779.
(8) Prifti, H.; Parasuraman, A.; Winardi, S.; Lim, T. M.; Skyllas-Kazacos, M. *Membranes* **2012**, *2*, 275−306.
(9) Leung, P.; Li, X.; Ponce de Leon, C.; Berlouis, L.; Low, C. T. J.; Walsh, F. C. *RSC Adv.* **2012**, *2*, 10125−10156.
(10) Wang, W.; Luo, Q. T.; Li, B.; Wei, X. L.; Li, L. Y.; Yang, Z. G. *Adv. Funct. Mater.* **2013**, *23*, 970−986.
(11) Skyllas-Kazacos, M.; Chakrabarti, M. H.; Hajimolana, S. A.; Mjalli, F. S.; Saleem, M. *J. Electrochem. Soc.* **2011**, *158*, R55−R79.
(12) Wei, X.; Nie, Z.; Luo, Q.; Li, B.; Sprenkle, V.; Wang, W. *J. Electrochem. Soc.* **2013**, *160*, A1215−A1218.
(13) Arora, P.; Zhang, Z. M. *Chem. Rev.* **2004**, *104*, 4419−4462.
(14) Belanger, S.; Stevenson, K. J.; Mudakha, S. A.; Hupp, J. T. *Langmuir* **1999**, *15*, 900−900.
(15) Zhang, H.; Zhang, H.; Li, X.; Mai, Z.; Zhang, J. *Energy Environ. Sci.* **2011**, *4*, 1676−1679.
(16) Li, B.; Luo, Q.; Wei, X.; Nie, Z.; Thomsen, E.; Chen, B.; Sprenkle, V.; Wang, W. *ChemSusChem* **2014**, *7*, 577−584.
(17) Wei, W.; Zhang, H.; Li, X.; Zhang, H.; Li, Y.; Vankelecom, I. *Phys. Chem. Chem. Phys.* **2013**, *2013*, 1766−1771.
(18) Zhang, H.; Zhang, H.; Li, X.; Mai, Z.; Wei, W. *Energy Environ. Sci.* **2012**, *5*, 6299−6303.
(19) Yang, R.; Xu, Z.; Yang, S.; Michos, I.; Li, L.-F.; Angelopoulos, A. P.; Dong, J. *J. Membr. Sci.* **2013**, *450*, 12−17.
(20) Zhang, H.; Zhang, H.; Zhang, F.; Li, X.; Li, Y.; Vankelecom, I. *Energy Environ. Sci.* **2013**, *2013*, 776−781.
(21) Smith, T. W.; Kuder, J. E.; Wychick, D. *J. Polym. Sci., Part A: Polym. Chem.* **1976**, *14*, 2433−2448.
(22) Flanagan, J. B.; Margel, S.; Bard, A. J.; Anson, F. C. *J. Am. Chem. Soc.* **1978**, *100*, 4248−4253.
(23) Saji, T.; Pasch, N. F.; Webber, S. E.; Bard, A. J. *J. Phys. Chem.* **1978**, *82*, 1101−1105.
(24) Moraes, J.; Ohno, K.; Gody, G.; Maschmeyer, T.; Perrier, S. *Beilstein J. Org. Chem.* **2013**, *9*, 1226−1234.
(25) Druta, I.; Avram, E.; Cozan, V. *Eur. Polym. J.* **2000**, *36*, 221−224.
(26) Vala, M. T.; Haebig, J.; Rice, S. A. *J. Chem. Phys.* **1965**, *43*, 886−897.
(27) Heinen, S.; Walder, L. *Angew. Chem., Int. Ed.* **2000**, *39*, 806−809.
(28) Baker, W. S.; Lemon, B. I.; Crooks, R. M. *J. Phys. Chem. B* **2001**, *105*, 8885−8894.
(29) Marchioni, F.; Venturi, M.; Ceroni, P.; Balzani, V.; Belohradsky, M.; Elizarov, A. M.; Tseng, H.-R.; Stoddart, J. F. *Chem.—Eur. J.* **2004**, *10*, 6361−6368.
(30) Palmore, G. T. R.; Smith, D. K.; Wrighton, M. S. *J. Phys. Chem. B* **1997**, *101*, 2437−2450.
(31) Bird, C. L.; Kuhn, A. T. *Chem. Soc. Rev.* **1981**, *10*, 49−82.
(32) Rodríguez-López, J.; Minguzzi, A.; Bard, A. J. *J. Phys. Chem. C* **2010**, *114*, 18645−18655.
(33) Wopschal, Rh; Shain, I. *Anal. Chem.* **1967**, *39*, 1514−1527.
(34) Laviron, E. *J. Electroanal. Chem.* **1979**, *101*, 19−28.
(35) Dalton, E. F.; Murray, R. W. *J. Phys. Chem.* **1991**, *95*, 6383−6389.
(36) Buttry, D. A.; Anson, F. C. *J. Am. Chem. Soc.* **1983**, *105*, 685−689.
(37) Paulson, S. C.; Okerlund, N. D.; White, H. S. *Anal. Chem.* **1996**, *68*, 581−584.
(38) Ragsdale, S. R.; White, H. S. *J. Electroanal. Chem.* **1997**, *432*, 199−203.
(39) Schwenzer, B.; Zhang, J.; Kim, S.; Li, L.; Liu, J.; Yang, Z. *ChemSusChem* **2011**, *4*, 1388−1406.
(40) Mai, Z.; Zhang, H.; Li, X.; Bi, C.; Dai, H. *J. Power Sources* **2011**, *196*, 482−487.
(41) Casassa, E. F. *J. Polym. Sci., Part C: Polym. Lett.* **1967**, *5*, 773−778.
(42) Degoulet, C.; Busnel, J. P.; Tassin, J. F. *Polymer* **1994**, *35*, 1957−1962.
(43) Renkin, E. M. *J. Gen. Physiol.* **1954**, *38*, 225−243.
(44) Meireles, M.; Bessieres, A.; Rogissart, I.; Aimar, P.; Sanchez, V. *J. Membr. Sci.* **1995**, *103*, 105−115.
(45) Wang, Y.; Teraoka, I.; Hansen, F. Y.; Peters, G. H.; Hassager, O. *Macromolecules* **2010**, *43*, 1651−1659.
(46) Phillip, W. A.; Amendt, M.; O'Neill, B.; Chen, L.; Hillmyer, M. A.; Cussler, E. L. *ACS Appl. Mater. Interfaces* **2009**, *1*, 472−480.
(47) Silva, V.; Pradanos, P.; Palacio, L.; Hernandez, A. *Desalination* **2009**, *245*, 606−613.
(48) Haraldsson, B.; Nystrom, J.; Deen, W. M. *Physiol. Rev.* **2008**, *88*, 451−487.
(49) Deen, W. M. *AlChE J.* **1987**, *33*, 1409−1425.
(50) Casassa, E. F.; Tagami, Y. *Macromolecules* **1969**, *2*, 14−26.
(51) Bohrer, M. P.; Deen, W. M.; Robertson, C. R.; Troy, J. L.; Brenner, B. M. *J. Gen. Physiol* **1979**, *74*, 583−593.
(52) Sun, C.; Chen, J.; Zhang, H.; Han, X.; Luo, Q. *J. Power Sources* **2010**, *195*, 890−897.
(53) Jia, C.; Liu, J.; Yan, C. *J. Power Sources* **2010**, *195*, 4380−4383.